Generation of approximate focus-wave-mode pulses from wide-band dynamic Gaussian apertures

Amr M. Shaarawi

Department of Engineering Physics and Mathematics, Faculty of Engineering, Cairo University, Giza, Egypt

Ioannis M. Besieris

Bradley Department of Electric Engineering, Virginia Polytechnic Institute and State University, Blacksburg, Virginia 24061

Richard W. Ziolkowski

Electromagnetics Laboratory, Department of Electrical and Computer Engineering, University of Arizona, Tuscon, Arizona 85721

Sherif M. Sedky

Department of Engineering Physics and Mathematics, Faculty of Engineering, Cairo University, Giza, Egypt

Received December 7, 1994; revised manuscript received March 14, 1995; accepted March 14, 1995

It is demonstrated that an approximation to the focus-wave-mode field can be generated from a dynamic Gaussian aperture. A source of this type is characterized by the time variation of its effective radius. The performance of such an aperture is studied in detail; it is demonstrated that the dynamic aperture shows a great enhancement over the corresponding static one. The types of source investigated provide an efficient scheme to launch narrow Gaussian pulses from extended apertures.

1. INTRODUCTION

In a recent study[1] concerning the causality and the evanescent components of the focus-wave-mode (FWM) solution to the scalar wave equation,[2,3] it was shown that, to address correctly the question of the launchability of such a wave, one should make a distinction between the source-free FWM field and a FWM pulse generated from an aperture. With the proper choice of parameters, it was confirmed that a good approximation of the exact FWM solution can be generated in a causal fashion from a dynamic Gaussian aperture.[1] The term dynamic aperture is used here in the sense that the effective radius of the aperture varies with time. It was shown that the FWM pulse generated from a causal dynamic infinite aperture situated at $z = 0$ does not spread out as it propagates into the $z > 0$ half-space. In contradistinction to the source-free FWM,[3] the field generated from a FWM dynamic Gaussian aperture is completely causal and does not have any acausality associated with it. For the source-free FWM pulse, one can select specific values for the various parameters characterizing the wave solution in such a way that the forward-going components of the pulse become dominant.[1,4,5] If a properly designed FWM solution is used to illuminate a dynamic aperture causally, its minuscule backward-traveling field components are turned into causal components that are still very weak and could be neglected for all practical purposes. For this reason the field generated by the dynamic aperture becomes a good approximation to the source-free FWM solution.

The generated approximation to the FWM pulse retains its shape for all times if the dynamic Gaussian aperture is excited for an infinitely long time.[1] The generating aperture thus needs an infinite amount of energy to be excited. However, the power needed to illuminate the aperture is *always* finite. Even when the aperture expands to an infinite size, the illuminating field becomes infinitesimally weak and tends to zero at the same rate at which the radius of the aperture approaches infinity. Within such a framework the generating aperture consumes an infinite amount of energy simply because it is excited for an infinitely long time. Thus, as far as we are concerned, there are no problems *per se* with the excitation of the FWM field except for the need of an infinite time to illuminate its aperture. Hence a dynamic Gaussian aperture excited for a long but finite period of time is expected to produce a field that is a good approximation to the original FWM solution. A detailed analysis of such an idea is the main purpose of this work.

The FWM belongs to a wider class of solutions[5–15] that have come to be called localized waves. Such pulsed fields exhibit extended ranges of localization and are characterized by their large bandwidths. Similarly, the initial illumination of the FWM aperture utilizes a wide-bandwidth field whose temporal- and spatial- frequency components are coupled together in a specific fashion. Such a coupling does not exist for quasi-monochromatic continuous-wave excitations. This extra freedom is enjoyed by all localized-wave (LW) solutions, in which a combination of the time-limited excitation of a specific LW pulse and the temporal–spatial distribution of the

0740-3232/95/091954-11$06.00

various elements constituting an aperture can have a direct effect on the spreading of the generated pulse. One should recall that a large number of the finite-energy LW pulses have been derived as a Laplace-type superposition of the original source-free FWM.[3,10,11] Additionally, certain guidelines for the design and performance of LW-driven dynamic apertures have been developed.[14] It has been shown that the coupling between the spatial- and temporal-frequency content of the excitation fields defined by the LW pulses is the main factor that determines the range of localization. The generation of such LW pulses has been verified experimentally with independently addressable ultrasonic array elements situated in a water tank.[16,17] In such experiments it has been confirmed that a specific LW solution, the modified-power-spectrum pulse,[11] can travel farther than a Gaussian pulse having the same transverse extension. Thus it has been established experimentally that specific pulses can do better than other ones even though they initially resemble one another, they are excited from the same aperture, and their source elements have the same frequencies.

Instead of using a superposition of FWM pulses to construct wide-band finite-energy LW pulses, we can alternatively excite the aperture with a FWM solution for a finite period of time. One should emphasize, however, that all finite-energy LW pulses are excited for a finite period of time. Nevertheless, such a property becomes quite evident in the approach that we adopted here by time windowing the infinite FWM excitation of the aperture. In this case, the field generated resembles the original FWM pulse closely. At the same time, the nature of the coupling between the spatial- and temporal-frequency content becomes clear because a dynamic Gaussian aperture at each time step represents a particular, regular, static Gaussian aperture. The static Gaussian aperture is a familiar object. Since we are advocating the possible use of wide-bandwidth time-limited pulses, the notion of a Rayleigh length separating the far from the near field becomes a little ambiguous. We do not have a specific carrier frequency for calculating the diffraction length as in the case of a continuous-wave quasi-monochromatic source. We simply claim that by varying the spatial- versus the temporal-frequency content of the source, one can generate pulses that can hold themselves better than others. To judge how far a pulse can propagate with very little deformation, we define the range of propagation as the distance from the aperture over which the amplitude of the centroid of the pulse decreases by a factor of one half. This is a specific way of determining how fast a pulse decays; one can then relate such a decay to the temporal and spatial bandwidths of the pulse. For the sake of enhancing the precision of our arguments, the indicated bandwidths will be characterized by their 3-dB points.

As indicated above, the FWM dynamic aperture has an effective radius that varies with time. For the specific case considered in this paper, the FWM aperture shrinks from its maximum radius at $t = -T$ to its smallest radius at $t = 0$ and then expands back to its initial size when $t = +T$. The power of the excitation field is always constant. The amplitude of the field illuminating the aperture becomes smallest (largest) when the radius of the aperture acquires its maximum (minimum) value. The focused portion of the generated pulse has a Gaussian profile whose radius equals the smallest radius of the aperture. As the aperture shrinks, it concentrates the power distributed on its largest area onto a spot characterized by its minimum radius. This concentration of the total power of the source onto a small spot can be perceived as a process of *temporal* focusing because it depends on how the size of the aperture varies with time. The range of such a highly focused central pulse also depends on the spatial–temporal distribution of the various elements constituting the source. Thus one can control the range and the power of the focus by temporally varying the sequence of the excitation of the various elements in a flat aperture. This approach should be contrasted with *spatial* focusing, which requires the construction of a curved aperture. In the spatial focusing case, the power is concentrated on a point far away from the source, and the range of the focal point can be altered only by varying the curvature of the elements of the aperture. The choice between a temporal and a spatial focusing scheme depends on the application of interest. A combination of the two focusing schemes could be quite advantageous; however, such a consideration is out of the scope of the present study.

In Section 2 we begin with the Fourier spectral content of the initial illumination of the FWM aperture. This will allow us to explain the nature of the coupling between the spatial- and the temporal-frequency components. The FWM initial field is then used in Section 3 to excite causally a flat aperture situated at the $z = 0$ plane for an infinitely long time. It will be shown that the field propagating in the $z > 0$ half-space closely resembles the original source-free FWM pulse, even though it is free from any acausal components. The generated FWM pulse travels for all times without spreading out. Since the generating aperture eventually becomes infinite in size, the Rayleigh limit is situated at an infinitely far distance from the aperture. However, when one studies the spectral content of the pulse it becomes clear that a delicate balance between the temporal-frequency components and the transverse spatial-frequency ones is responsible for holding the pulse together for all times. It is the aim of this study to investigate what happens to such a balance when the FWM aperture is excited for a finite period of time. It will be shown that the pulse starts to spread out at finite distances, the range of propagation depending on the period of excitation, the smallest radius of the aperture, and the 3-dB cutoff of the temporal-frequency spectrum. Such a result agrees with the diffraction limit predicted by Hafizi and Sprangle.[18] The Hafizi–Sprangle limit beats by far the Rayleigh length of a narrow Gaussian excited from a large static aperture. The finite-time dynamic FWM aperture thus provides an interesting scheme for propagating narrow Gaussian-like pulses from extended apertures of much larger dimensions. The Gaussian pulses generated from a finite-time FWM aperture travel with little dispersion for distances several orders of magnitude larger than similar narrow Gaussians launched from static apertures of the same size and utilizing the same maximum frequency.

2. SPECTRAL CONTENT OF THE EXCITATION OF THE INFINITE FWM APERTURE

It has been shown previously[1,5] that a Huygens construction of a Bessel beam[19] generated from an infinite aperture cancels out all acausal incoming components, and the Bessel beam is propagated invariantly away from the aperture. Since the FWM can be considered a superposition of Bessel beams,[1,4] the same approach ensures that no acausal incoming fields are contributing to the FWM-generated field. We start by defining the initial FWM field illuminating an aperture situated at the $z = 0$ plane. The field is the real part of the azimuthally symmetric complex FWM pulse; specifically,

$$\Psi_i(\rho, t) = \mathrm{Re}\left\{ \frac{1}{(a_1 - ict)} \times \exp[-\beta\rho^2/(a_1 - ict)]\exp(i\beta ct)\right\}. \quad (2.1)$$

Because of the first exponential term on the right-hand side of Eq. (2.1), the field exists mainly inside the radius:

$$R(t) = \frac{|ct|}{\sqrt{\beta a_1}} \qquad \text{for } ct \gg a_1 . \quad (2.2)$$

It is clear that such a time-varying radius becomes infinite when $ct = \pm\infty$. It decreases from an infinite value to a radius $R(t) \sim \sqrt{a_1/\beta}$ when t approaches the value of zero, and henceforth it expands toward an infinite size. Furthermore, it can be deduced from Eq. (2.1) that the field amplitude varies as $1/ct$ for $ct \to \infty$. Subsequently the power density decreases as $(1/ct)^2$ and becomes equal to zero at $t = \pm\infty$. This means that as $ct \to \infty$ the total power of the field illuminating the aperture (the intensity of the field $\times$ the area of the aperture) remains constant. This behavior should be compared with the illumination of infinite apertures by plane waves or Bessel beams. In these two cases we need infinite power to illuminate the corresponding apertures. From Eq. (2.2) it can be seen that the parameter βa_1 controls the speed v_{ap} of the shrinking and expanding of the aperture, where

$$v_{ap} = \frac{c}{\sqrt{\beta a_1}} \qquad \text{for } ct \gg a_1 . \quad (2.3)$$

It has been previously shown[1,4,5] that the quantity βa_1 determines whether the field of the source-free FWM is dominated by forward- or backward-traveling field components. The case of $\beta a_1 > 1$ has been considered by Heyman[20] and Felsen (see Ref. 21), who proved that under such a condition the FWM field is dominated by its acausal components. The other limit, for which $\beta a_1 \ll 1$, has been considered by the present authors. We have shown that the forward-traveling field components of the source-free FWM are dominant when $\beta a_1 \ll 1$ (Refs. 1 and 4) and that one can neglect the minuscule backward-propagating components without effectively altering the shape of the FWM pulse. We are interested primarily in the latter case, in which the causal (forward-traveling) components are the major contributors to the FWM field generated from a dynamic Gaussian aperture. According to Eq. (2.3) the FWM aperture expands effectively at a speed $v_{ap} > c$ when $\beta a_1 < 1$. One achieves this practically by composing the aperture from separately excitable elements. This was the case for the arrays used in experiments performed to establish the launchability of other LW solutions.[16,17]

The Fourier spectrum of the illumination of the FWM aperture is calculated from the Fourier transform of Eq. (2.1), viz.,

$$\Phi(\chi, \omega) = \int_{-\infty}^{\infty} dt \int_0^{\infty} d\rho\rho J_0(\chi\rho)\exp(-i\omega t)\frac{1}{(a_1 - ict)} \times \exp[-\beta\rho^2/(a_1 - ict)]\exp(i\beta ct). \quad (2.4)$$

The integrations over t and ρ when carried out yield

$$\Phi(\chi, \omega) = \frac{\pi}{\beta}\delta\{\omega - [(\chi^2/4\beta) + \beta]c\}\exp[-(\chi^2/4\beta)a_1]. \quad (2.5)$$

The temporal- and spectral-frequency contents can now be calculated from the inverse Fourier transform of the spectrum given in Eq. (2.5) with respect to χ and ω, respectively. Starting with the temporal-frequency components, one obtains

$$\Phi_t(\rho, \omega) = \frac{\pi}{\beta}\int_0^{\infty} d\chi\chi J_0(\chi\rho)\delta\{\omega - [(\chi^2/4\beta) + \beta]c\} \times \exp[-(\chi^2/4\beta)a_1], \quad (2.6)$$

which gives

$$\Phi_t(\rho, \omega) = 2\pi J_0\{2\rho\sqrt{\beta[(\omega/c) - \beta]}\} \times \exp[-(\omega/c)a_1]\exp(\beta a_1)\mathbb{H}[(\omega/c) - \beta], \quad (2.7)$$

where $\mathbb{H}[(\omega/c) - \beta]$ is the Heaviside unit-step function. Notice that the factor $\exp(\beta a_1)$ determines how large the contribution of the spectral-frequency components is. For $\beta a_1 \ll 1$, the factor $\exp(\beta a_1) \sim 1$ does not affect the shape of the temporal spectrum. On the other hand, when $\beta a_1 > 1$, the factor $\exp(\beta a_1)$ becomes significant because it balances out the exponential decay $\exp[-(\omega/c)a_1]$ in the temporal-frequency spectrum. Even though the 3-dB point seems to lie at $(\omega/c) \sim 1/a_1$, there could still be significant components contributing to the spectrum because of the factor $\exp(\beta a_1) \gg 1$. Hence we have to extend the maximum radial frequency to

$$\omega_{\max} \sim (4/a_1 + \beta)c . \quad (2.8)$$

The above expression sheds more light on the significance of the two conditions $\beta a_1 \ll 1$ and $\beta a_1 > 1$. The first condition corresponds to the case in which $\omega_{\max} \sim 4\omega_{3\,\mathrm{db}} = 4c/a_1$, and most of our bandwidth is supplied by the temporal components. With $\beta a_1 > 1$, the maximum angular frequency is given by $\omega_{\max} \sim [(4/a_1) + \beta]c > 4\omega_{3\,\mathrm{db}}$. Such an increase in the significant temporal-frequency components arises because of the increase in the contributions of the spatial-frequency spectrum. As indicated above, such an increase is expressed by the existence of the factor $\exp(\beta a_1) \gg 1$. Recalling that in Eq. (2.7) $\omega_{\min} = \beta c > c/a_1$, we see that the temporal-frequency bandwidth becomes very narrow and exists mainly in the

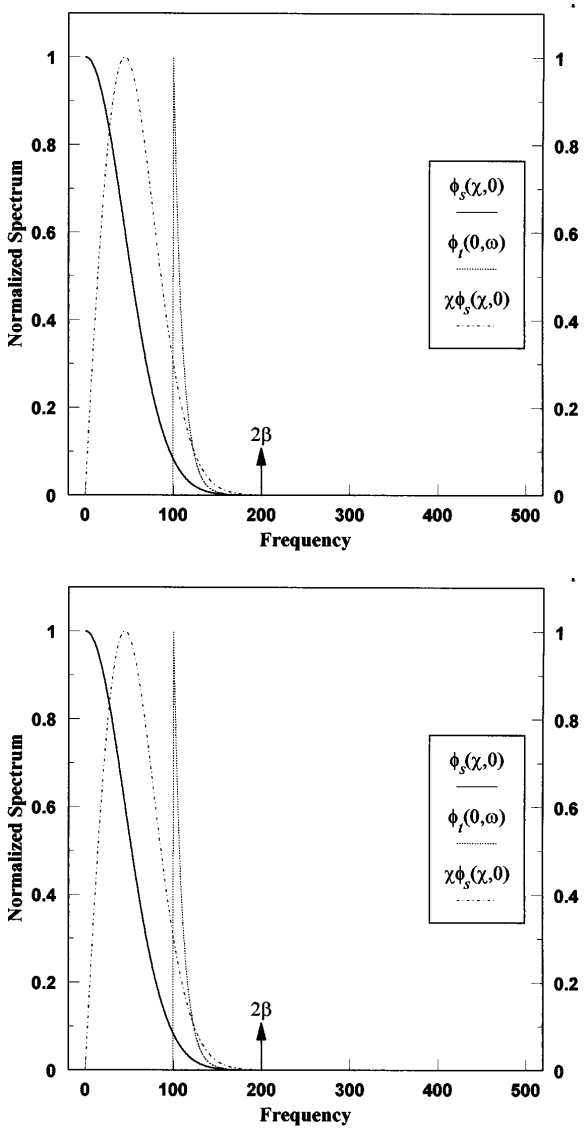

Fig. 1. Temporal and spatial spectral content for FWM aperture illumination when $\beta a_1 > 1$.

tail of the exponential $\exp[-(\omega/c)a_1]$. Such a narrowing of the temporal-frequency content could be perceived as a depletion of the temporal frequencies on behalf of the spatial ones, which supply most of the power to the generating field.

In the same vein, the spatial-frequency components can be calculated from the inverse Fourier transform of Eq. (2.5) with respect to ω, where

$$\Phi_s(\chi, t) = \frac{1}{2\pi} \int_{-\infty}^{\infty} d\omega \, \frac{\pi}{\beta} \, \delta\{\omega - [(\chi^2/4\beta) + \beta]c\} \times \exp[-(\chi^2/4\beta)a_1]\exp(i\omega t) \tag{2.9}$$

gives

$$\Phi_s(\chi, t) = \frac{1}{2\beta} \exp[-(\chi^2/4\beta)a_1]\exp\{i[(\chi^2/4\beta) + \beta]ct\}. \tag{2.10}$$

The bandwidth of the spatial spectrum is controlled by the quantity $\sqrt{\beta/a_1}$, which is the inverse of the smallest radius of the aperture or, equivalently, the radius of the highly focused central Gaussian launched by the FWM aperture. For $\beta a_1 > 1$ we have $\sqrt{\beta/a_1} > 1/a_1$; this indicates that spatial bandwidth is greater than the temporal one, as shown in Fig. 1. Similarly, the condition $\beta a_1 \ll 1$ indicates that $\sqrt{\beta/a_1} \ll 1/a_1$. Consequently, the main contributions to the excitation field come from the temporal spectral components in that limit. This behavior is illustrated in Fig. 2. In Figs. 1 and 2 we have plotted examples of the normalized spatial- and temporal-frequency spectra in the two limits $\beta a_1 > 1$ and $\beta a_1 \ll 1$, respectively. The parameters β and a_1 in Fig. 1 have been chosen to equal 100 and 0.1, respectively. In Fig. 2 we have chosen $\beta = 10$ and $a_1 = 0.01$. The choice of the values of the parameters is a matter of convenience; we picked the indicated values to ensure that the spatial spectrum would have the same bandwidth in both cases. For $\beta a_1 = 10$, Fig. 1 shows that the temporal-frequency content becomes thin and exists only at the tail of the spatial spectrum. Notice that in Eq. (2.8), $(4/a_1) = 40 < \beta$, which is equal to the low-frequency cutoff point of the temporal components as indicated by the Heaviside unit-step function in Eq. (2.7). The temporal-frequency components are thus depleted, and the temporal- and spatial-frequency components become decoupled from each other. In contrast, when $\beta a_1 = 0.1$, the temporal spectrum becomes much broader and overlaps most of the spatial components. Finally, we note that the markers placed at 2β in the two figures will be helpful below when we discuss the similarity between the causal field generated from a dynamic Gaussian aperture and that generated from the source-free FWM.

3. PROPAGATION OF THE FWM FIELD IN THE $z > 0$ HALF-SPACE

The initial field defined on the aperture [see Eq. (2.1)] is a superposition of Bessel beams[19] at the plane $z = 0$; specifically,

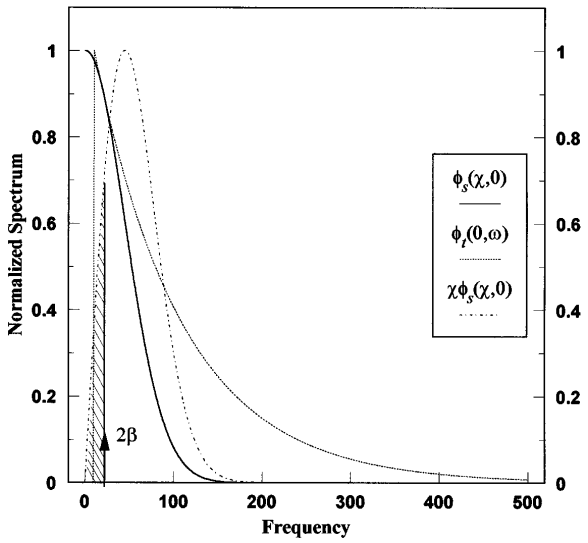

Fig. 2. Temporal and spatial spectral content for FWM aperture illumination when $\beta a_1 < 1$.

$$\Psi_i(\rho, t) = \left\{ \frac{1}{2\pi} \int_0^\infty d\chi \chi J_0(\chi\rho) \int_0^\infty d\omega \Phi(\chi, \omega) \times \exp[-i\sqrt{(\omega/c)^2 - \chi^2}\, z]\exp(i\omega t) \right\}_{z=0} . \quad (3.1)$$

The normal derivative of this field on the aperture is evaluated before we set $z = 0$. Consequently, we restrict the quantity $\sqrt{(\omega/c)^2 - \chi^2}$ to positive values only, to ensure the forward illumination of the aperture. Notice also that ω is restricted to positive values if β is positive. This follows from the roots of the δ function in the spectrum given in Eq. (2.5).

In order to calculate the outgoing field propagating into the $z > 0$ half-space, we utilize Huygens's construction.[22] Accordingly, the field at a point $\mathbf{R}$ and time t inside a wave-front surface having a zero field outside such a surface is given by the integration over the area of the infinite aperture. Such a construction is expressed in the following mathematical form[22]:

$$\Psi(\rho, z, t) = \frac{1}{4\pi} \int_0^{2\pi} d\phi' \int_0^\infty d\rho' \frac{\rho'}{R} \left[-\partial_{z'} \Psi(\rho', z' = 0, t') + \frac{z}{R^2} \Psi(\rho', z' = 0, t') + \frac{z}{cR} \partial_{t'} \Psi(\rho', z' = 0, t') \right]_{t' = t - R/c} . \quad (3.2)$$

The primed coordinates refer to source points on the aperture, and the unprimed ones refer to the observation points in the $z > 0$ half-space. Substituting for the initial excitation given in Eq. (3.1) and making use of the identity[5]

$$\partial_z \left[\frac{\exp(-i\omega R/c)}{R} \right] = -\left(\frac{z}{R^3} + i \frac{\omega z}{cR^2} \right) \exp(-i\omega R/c),$$

we get

$$\Psi(\rho, z, t) = \frac{1}{4\pi} \int_0^{2\pi} d\phi' \int_0^\infty d\rho' \frac{\rho'}{2\pi} \int_0^\infty d\chi \chi J_0(\chi\rho') \times \int_0^\infty d\omega \Phi(\chi, \omega)\exp(i\omega t) \times \left\{ i\sqrt{(\omega/c)^2 - \chi^2}\, \frac{\exp(-i\omega R/c)}{R} - \partial_z \left[\frac{\exp(-i\omega R/c)}{R} \right] \right\}. \quad (3.3)$$

Here $R = (\rho'^2 + \rho^2 - 2\rho'\rho \cos \phi' + z^2)^{1/2}$. Since the square root $\sqrt{(\omega/c)^2 - \chi^2}$ is always positive, it forces the bracketed term in Eq. (3.3) to pick up only outgoing waves and to cancel out any waves converging on the aperture. To justify such a claim one can start with the identity

$$\frac{\exp(-i\omega R/c)}{R} = \frac{1}{\pi} \int_0^\infty d\lambda \int_{-\infty}^\infty d\kappa_z \lambda J_0(\lambda\rho^*) \times \frac{\exp(-ik_z z)}{\kappa_z^2 - [(\omega/c)^2 - \lambda^2]} \quad (3.4)$$

to evaluate the bracketed term in Eq. (3.3). Here $\rho^* = (\rho'^2 + \rho^2 - 2\rho'\rho \cos \phi')^{1/2}$, and the contour of integration Γ in the complex κ_z plane is shown in Fig. 3. For $(\omega/c) > \lambda$ the contour of integration is closed in the lower half-plane to ensure the integrability of Eq. (3.4) for $z > 0$. For $(\omega/c) < \lambda$ the analysis becomes more complicated because the δ function in the spectrum given in Eq. (2.5) forces ω to become complex. Such a situation was dealt with in detail in another study[1] that was concerned primarily with the evanescent-field components on an infinite FWM aperture. In that study it was shown that there are no evanescent fields associated with an infinite FWM aperture. On carrying out the contour integration over the κ_z variable and taking the partial derivative with respect to z, we get

$$\partial_z \left[\frac{\exp(-i\omega R/c)}{R} \right] = -\int_0^\infty d\lambda \lambda J_0(\lambda\rho^*) \times \exp[-i\sqrt{(\omega/c)^2 - \lambda^2}\, z] - \int_0^\infty d\lambda \lambda J_0(\lambda\rho^*) \times \exp[+i\sqrt{(\omega/c)^2 - \lambda^2}\, z]. \quad (3.5)$$

From the *a priori* knowledge of the appearance of $\delta(\lambda - \chi)$ [see Eq. (3.7) below], the bracketed term in Eq. (3.3) becomes

$$\left\{ i\sqrt{(\omega/c)^2 - \chi^2}\, \frac{\exp(-i\omega R/c)}{R} - \partial_z \left[\frac{\exp(-i\omega R/c)}{R} \right] \right\} = 2 \int_0^\infty d\lambda \lambda J_0(\lambda\rho^*)\exp[-i\sqrt{(\omega/c)^2 - \lambda^2}\, z]. \quad (3.6)$$

Thus the acausal components converging on the aperture are filtered out. This is a direct consequence of the forward illumination of the FWM aperture, viz., the restriction of $\sqrt{(\omega/c)^2 - \chi^2}$ in Eq. (3.3) to positive values only. Following the same procedure as in App. B of Ref. 5, we

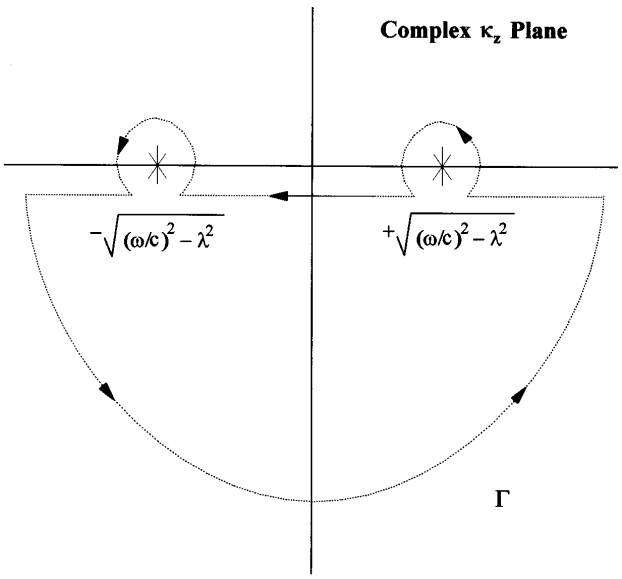

Fig. 3. Contour of integration Γ in the complex κ_z plane used for evaluation of the integration in Eq. (3.4).

can use the addition theorem of the Bessel function[23] together with Eq. (3.6) to rewrite Eq. (3.3) as follows:

$$\Psi(\rho, z, t) = \frac{1}{2\pi}\int_0^\infty d\rho'\rho'\int_0^\infty d\chi\chi J_0(\chi\rho') \times \int_0^\infty d\omega\Phi(\chi, \omega)\exp(i\omega t) \times \int_0^\infty d\lambda\lambda J_0(\lambda\rho)J_0(\lambda\rho') \times \exp[-i\sqrt{(\omega/c)^2 - \lambda^2}\, z]. \quad (3.7)$$

One can evaluate the integration over ρ' by using the orthogonality of the Bessel function, which gives a $\delta(\lambda - \chi)$ term. Thus the integration over ρ' and λ reduces Eq. (3.7) to

$$\Psi(\rho, z, t) = \frac{1}{2\beta}\int_0^\infty d\chi\chi J_0(\chi\rho) \times \int_0^\infty d\omega\delta\{\omega - [(\chi^2/4\beta) + \beta]c\} \times \exp[-(\chi^2/4\beta)a_1] \times \exp(i\omega t)\exp[-i\sqrt{(\omega/c)^2 - \chi^2}\, z]. \quad (3.8)$$

For $(\omega/c) = [(\chi^2/4\beta) + \beta]$, the square root $\sqrt{(\omega/c)^2 - \chi^2}$ would acquire the value of either $[(\chi^2/4\beta) - \beta]$ or $-[(\chi^2/\beta) - \beta]$, depending on whether $\chi > 2\beta$ or $\chi < 2\beta$, respectively. This is the case because only positive values of the square root give nonzero contributions, as we have shown in Eq. (3.6). One can then easily carry the integration over ω to obtain

$$\Psi(\rho, z, t) = \frac{1}{2\beta}\int_0^{2\beta} d\chi\chi J_0(\chi\rho)\exp[-(\chi^2/4\beta)a_1] \times \exp[i(\chi^2/4\beta)(z + ct)]\exp[-i\beta(z - ct)] + \frac{1}{2\beta}\int_{2\beta}^\infty d\chi\chi J_0(\chi\rho)\exp[-(\chi^2/4\beta)a_1] \times \exp[-i(\chi^2/4\beta)(z - ct)]\exp[i\beta(z + ct)]. \quad (3.9)$$

For $\beta a_1 \ll 1$ we have an aperture that apparently shrinks and expands at speeds greater than that of light. As shown in Fig. 2, the 3-dB point of the χ spectrum $2\sqrt{\beta/a_1} \gg 2\beta$. Thus we can rewrite Eq. (3.9) as

$$\Psi(\rho, z, t) = \frac{i}{\beta}\int_0^{2\beta} d\chi\chi J_0(\chi\rho)\exp[-(\chi^2/4\beta)a_1] \times \sin\{[(\chi^2/4\beta) - \beta]z\}\exp\{i[(\chi^2/4\beta) + \beta]ct\} + \frac{1}{2\beta}\int_0^\infty d\chi\chi J_0(\chi\rho)\exp[-(\chi^2/4\beta)a_1] \times \exp[-i(\chi^2/4\beta)(z - ct)]\exp[i\beta(z + ct)]. \quad (3.10)$$

The integration of the second term on the right-hand side of Eq. (3.10) yields the source-free FWM pulse. The first integral, however, is carried out over a narrow portion of the total bandwidth of the χ spectrum. In fact, the ratio between the area $2\pi\int\chi d\chi \sim 0(\pi\chi^2)$ with the proper limits of integration taken into consideration results in an estimate of the relative magnitude of the first term in Eq. (3.10) in comparison with the second. Specifically, the amplitude of the first term is of order $(2\beta)^2/(2\sqrt{\beta/a_1})^2 = 0(\beta a_1)$ relative to that of the center of the FWM pulse. Thus the first term is algebraically small in comparison with the second; and, for all practical purposes, the field generated by the aperture would closely resemble the source-free FWM pulse. The same result could be deduced directly from Fig. 2, in which the first integration gives the area of the shaded triangle under the $\chi\Phi_s(\chi)$ curve. The second integration is the area under the whole $\chi\Phi_s(\chi)$ curve. The ratio of the two areas is $0(\beta a_1)$.

A time sequence of the generation of the FWM pulse from an infinite-time dynamic aperture is shown in Fig. 4. For negative times the aperture generates a precursor field of low intensity, which is not focused at all. The focused waist of the pulse is formed at $t = 0$ when the aperture shrinks to its smallest radius. As the aperture starts expanding, the amplitude of the focused centroid is sustained as long as the aperture is allowed to expand to an infinite size. In Fig. 4 the contours of the generated field have intensities that are 0.6, 0.4, 0.2, and 0.02 relative to the intensities at the central line of propagation. For positive times the highest intensity exists at the focused centroid, which has the highest density of lines. As we move along the central line away from the centroid, the contour lines open up and their densities decrease, indicating that we have broader Gaussians with smaller amplitudes.

4. FINITE-TIME EXCITATION OF THE DYNAMIC FWM APERTURE

In this section we investigate the consequences of cutting off the expansion time of the FWM aperture at a finite value. We can do this by introducing a Gaussian time window of width $2T$; specifically, the spectrum content of the excitation field can be calculated as

$$\Phi(\chi, \omega) = \int_{-\infty}^\infty dt\int_0^\infty d\rho\rho J_0(\chi\rho)\exp(-i\omega t) \times \frac{1}{(a_1 - ict)}\exp[-\beta\rho^2/(a_1 - ict)] \times \exp(i\beta ct)\exp(-t^2/4T^2). \quad (4.1)$$

Here the Gaussian window allows the aperture to expand effectively only from $t = -T \to +T$. The spectrum of the field illuminating the aperture becomes

$$\Phi(\chi, \omega) = \frac{\pi}{\beta c}\hat{\delta}\{(\omega/c) - [(\chi^2/4\beta) + \beta]; cT\} \times \exp[-(\chi^2/4\beta)a_1], \quad (4.2)$$

where

$$\hat{\delta}\{(\omega/c) - [(\chi^2/4\beta) + \beta]; cT\} = \frac{cT}{\sqrt{\pi}}\exp(-(cT)^2\{(\omega/c) - [(\chi^2/4\beta) + \beta]\}^2). \quad (4.3)$$

In the limit $T \to \infty$, the Gaussian $\hat{\delta}$ function goes to the Dirac δ function that characterizes the spectrum of the infinite-time excitation [see Eq. (2.5)]. When cT is large, the Gaussian in spectrum (4.2) reduces to a narrow distribution with a very small bandwidth for which $(\omega/c) \sim [(\chi^2/4\beta) + \beta]$ provides most of the significant

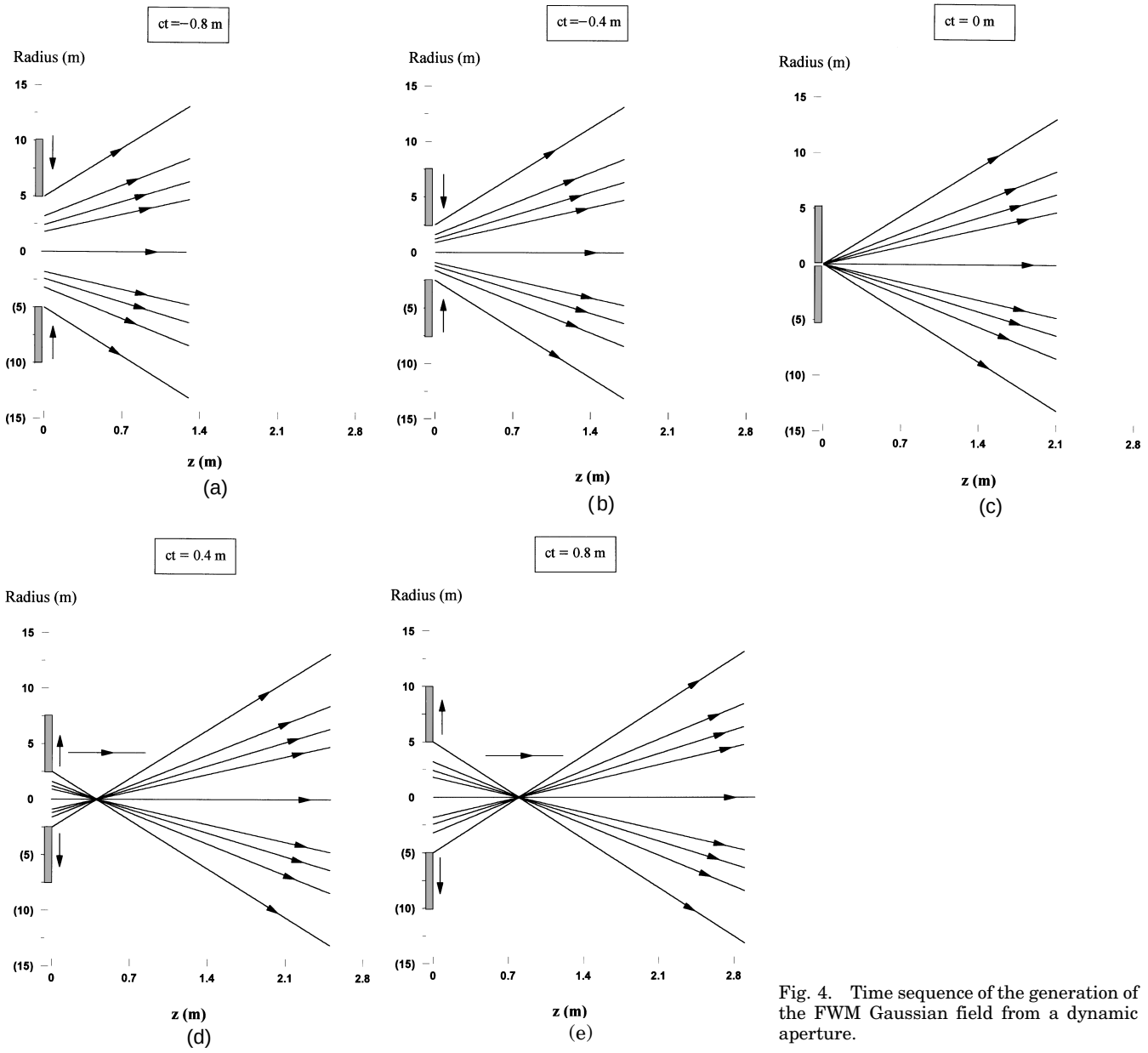

Fig. 4. Time sequence of the generation of the FWM Gaussian field from a dynamic aperture.

contributions to the spectrum. Thus we have a narrow Gaussian centered around $(\omega/c) = [(\chi^2/4\beta) + \beta]$ that sweeps across the whole χ spectrum as χ is varied from 0 to $4\sqrt{\beta/a_1}$. We demonstrated in Section 2 that, for $\beta a_1 \ll 1$, the portion of the spectrum for which $\chi < 2\beta$ is negligible for all practical purposes. The same applies for the case of a narrow Gaussian spectrum such as that given in Eq. (4.2). If we follow the same procedure as that described in Section 3, the field generated in the $z > 0$ half-space can be calculated as

$$\Psi(\rho, z, t) = \frac{1}{2\beta} \int_0^\infty d\chi \chi J_0(\chi\rho) \times \int_0^\infty d\kappa \hat{\delta}\{\kappa - [(\chi^2/4\beta) + \beta]; cT\} \times \exp[-(\chi^2/4\beta)a_1]\exp(i\kappa ct) \times \exp(-i\sqrt{k^2 - \chi^2}\, z), \quad (4.4)$$

where $\kappa = \omega/c$. The square root $\sqrt{k^2 - \chi^2}$ acquires only positive values to ensure that all the field components are diverging from the aperture. To study the decay pattern of the field given in Eq. (4.4), we shall concentrate on the centroid of the pulse at $z = ct$ for $t > 0$. For the field generated from an infinite aperture [see the second term in Eq. (3.10)] the Dirac δ function in the spectrum forces the phase $[(\omega/c) - \sqrt{(\omega/c)^2 - \chi^2}\,]z = 2\beta z$ to be independent of χ. Hence the centroid propagates to infinite distances from the aperture without any decay and varies sinusoidally only over distances that are integer multiples of π/β. Now, for the finite aperture such a delicate balance does not exist. Even though the phase $(\kappa - \sqrt{\kappa^2 - \chi^2})z \sim 2\beta z$, the Gaussian $\hat{\delta}$ function nevertheless introduces small deviations that are dependent on both χ and z. For large values of z the exponential term becomes highly oscillatory over large portions of the χ spectrum. On integration, such high oscillations progressively remove significant portions of the χ spectrum

as z is increased. Consequently, the amplitude of the centroid of the generated pulse decreases as it propagates away from the aperture.

We evaluate the integration in Eq. (4.4), for which $z = ct$ and $\rho = 0$, numerically to determine how fast the amplitude of the centroid decays in the positive z direction as the pulse propagates away from the aperture. Because the integrand in Eq. (4.4) can become highly oscillatory, especially for large values of z, a double integration over χ and κ might be quite tedious. Nevertheless, the Gaussian $\hat{\delta}\{\kappa - [(\chi^2/4\beta) + \beta]; cT\}$ becomes very narrow for $\beta cT \gg 1$. Therefore, instead of having an infinite range of integration over κ from 0 to ∞, we effectively have a finite range that we have chosen to vary from $[(\chi^2/4\beta) + \beta - (4/cT)]$ to $[(\chi^2/4\beta) + \beta + (4/cT)]$. All significant contributions to the κ integration comes from this finite κ window. Subsequently, the computation of the double integration is greatly simplified. This κ window sweeps the χ spectrum as χ is varied over the whole bandwidth. One should note, however, that the deviation of $(\kappa - \sqrt{\kappa^2 - \chi^2})$ from 2β is larger for smaller values of χ. As a consequence, the integrand in Eq. (4.4) becomes highly oscillatory inside the κ windows covering the lower portions of the χ spectrum. As z is increased, the oscillations of the integrand progressively remove larger portions of the χ-frequency components. Hence the integration in Eq. (4.4) results in a Gaussian pulse, the centroid of which decreases in amplitude as it travels forward in the positive z direction.

The numerical evaluation of Eq. (4.4) is shown in Figs. 5 and 6, in which the normalized amplitudes of the centroid are plotted at various distances $z = ct \geq 0$. The amplitude is normalized relative to that of the centroid of the pulse as it goes through the aperture at $z = ct = 0$. The parameters used in the numerical integration have been chosen to comply with the conditions required for the generated pulse to resemble the source-free FWM; specifically, we need $\beta a_1 \ll 1$ and $\beta cT \gg 1$. Toward this end in Fig. 5 we have chosen $\beta = 400\ \mathrm{m}^{-1}$ and $a_1 = 4 \times 10^{-7}$ m. This choice of parameters produces a Gaussian of radius $w_0 = \sqrt{a_1/\beta} = 3.162 \times 10^{-5}$ m, which is approximately the smallest radius acquired by the aperture. In Fig. 5 the amplitude of the centroid, calculated from the real part of integration (4.4), has been plotted for various $z = ct > 0$ points. Three curves are shown in the figure, each one characterized by a specific cT value. From Eq. (2.2) it can be seen that the value of cT determines the largest radius acquired by the aperture, namely, $R_{\max} = cT/\sqrt{\beta a_1}$. In Fig. 5 the smallest aperture radius w_0 is kept constant, while one varies $R_{\max}$ by choosing $cT = 0.13$, 0.26, and 0.52 m. Thus when the dynamic FWM aperture is allowed to expand for longer times, it acquires larger radii. Keeping β and a_1 constant for the three plotted curves means that the bandwidths of the spatial and the temporal spectra (see Fig. 2) are the same for all three cases. A comparison of the decay patterns of the centroid for each cT value indicates that the amplitude of the centroid falls off at a slower rate as $R_{\max}$ is increased. Notice that the amplitude reaches half its aperture value at distances that double as the maximum radius is increased to twice its original value. This shows that the range of the pulse varies linearly with the largest radius of the aperture. Such behavior has been alluded to by Hafizi and Sprangle[18] in their attempt to define a diffraction length of the LW fields as they propagate away from their generating apertures. The same results agree with the guidelines deduced in Ref. 24 for the design of LW's. At this point one should note that the amplitude of the centroid is calculated at multiples of $z = 50\pi$ m. Such an amplitude varies sinusoidally along the z direction with its maxima occurring when $2\beta z$ is an integer multiple of 2π. This is typical behavior of a field propagating within the Rayleigh diffraction length characterizing its source. Thus one should bear in mind that in Fig. 5 there are 20,000 cycles between any two displayed points. Each of these points is the maximum of its own cycle.

The value of the minimum radius w_0 is varied in Fig. 6, while the maximum radius $R_{\max}$ is kept unchanged. To keep the same maximum frequency of the source for all three cases, we assigned the parameter a_1 the constant value 4×10^{-7} m. Furthermore, we chose the following

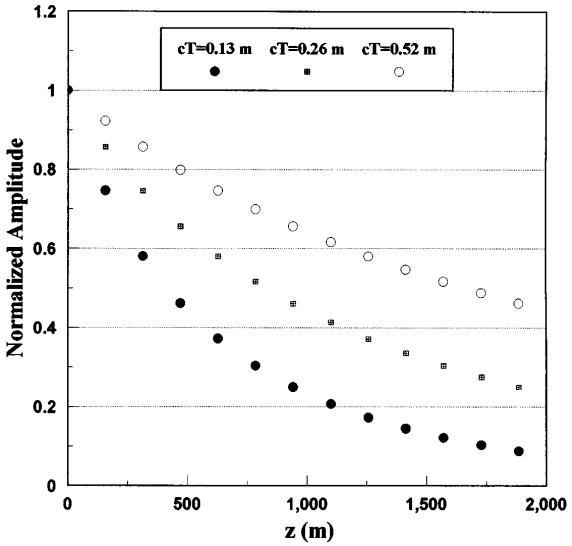

Fig. 5. Decay in the centroid of the Gaussian pulse as a function of distance z from the aperture as cT is varied.

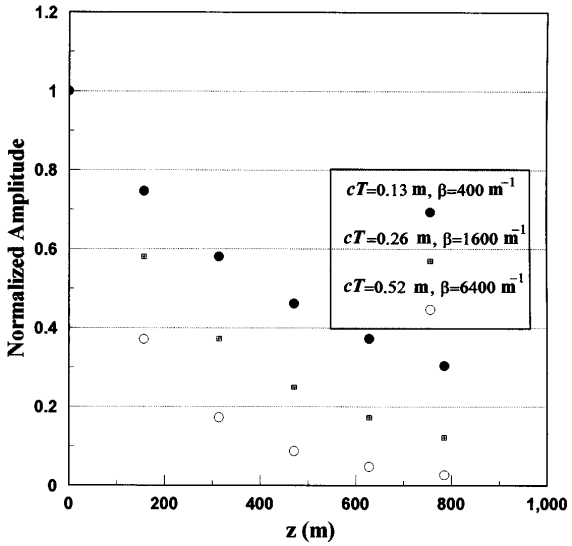

Fig. 6. Decay in the centroid of the Gaussian pulse as a function of distance z from the aperture as w_0 is varied.

parameter values for the three cases considered in Fig. 6: $\beta = 400$, 1600, and 6400 m^{-1} and $cT = 0.13$, 0.26, and 0.52 m, respectively. For these parameter values $R_{max} = 10.277$ m, and $w_0 = 3.162 \times 10^{-5}$, 1.581×10^{-5}, and 7.9×10^{-6} m. It is straightforward to deduce from Fig. 6 that when a_1 is kept constant (i.e., the maximum frequency is kept the same in all three cases) the centroid decays at a faster rate as w_0 is decreased. Again one can assert that the range of the pulse decreases linearly with w_0, which is another property predicted by the analysis in Ref. 24 and agrees nicely with the diffraction limit estimated by Hafizi and Sprangle.[18]

At this stage we need to further our understanding of the behavior of dynamic apertures in relation to the diffraction length estimated by Hafizi and Sprangle.[18] In an effort to define a diffraction length for LW fields, they estimated the angular spread of the radiation relative to the normal to the aperture as $\Delta\chi/\kappa$. For the dynamic aperture under consideration, the transverse wave-number spread $\Delta\chi$ can be taken equal to $2\sqrt{\beta/a_1}$, and $k = \omega/c$ is equal to $1/a_1$. Notice that such values are well above the corresponding 3-dB points of the χ and the ω spectra. From the above definition of the angular spread of the radiation as it emerges from the aperture, Hafizi and Sprangle deduced the following diffraction length[18]:

$$z_{HS} = \frac{R\kappa}{\Delta\chi}, \tag{4.5}$$

where R is the radius of the aperture (for a dynamic aperture one should take $R = R_{max}$) and HS stands for Hafizi and Sprangle. Hafizi and Sprangle have made the correct observation that the diffraction length associated with a specific LW field depends linearly on the radius of the central pulse w_0. The modified-power-spectrum pulse (which has been extensively studied in Ref. 11) resembles the FWM closely; hence it can also be generated by an aperture that effectively changes its size. Consequently, the behavior of a pulse launched from a finite-time FWM aperture (similarly to the modified-power-spectrum pulse) relies heavily on its dynamic character. We already know that the FWM spectral spread $\Delta\chi$ is related directly to the radius of the central Gaussian pulse $w_0 = R_{min} = \sqrt{a_1/\beta}$. Therefore the Hafizi–Sprangle diffraction limit can be rewritten as

$$z_{HS} = \frac{R_{max}R_{min}}{2a_1}. \tag{4.6}$$

Thus the diffraction length of a dynamic aperture depends on its largest and smallest radii and on the bandwidth of its signal generator. The latter is characterized by the quantity $1/a_1$. For the FWM aperture we can substitute for R_{max} and R_{min} in terms of the parameters β and a_1 to obtain $z_{HS} = cT/2\beta a_1$. If we substitute for the values of the parameters cT, β, and a_1 used in Fig. 5, we obtain $z_{HS} = 406$, 812, and 1624 m, respectively. Such values agree nicely with the computed half-amplitude ranges as illustrated in Fig. 5.

One should emphasize, however, that the cyclic behavior of the amplitude as a function of z persists even for distances larger than z_{HS}. This is the case because we are in the near-field region of a *static* aperture of radius R_{max} whose Rayleigh length $z_R = \pi R_{max}^2/\lambda$ is greater than z_{HS} defined above. On the other hand, the ranges deduced from Fig. 5 are well inside the far-field region of an aperture whose effective radius is that of the Gaussian pulse w_0, for which $z_R = \pi w_0^2/\lambda$. The way in which a pulse behaves between those two diffraction-length scales depends primarily on the temporal- and spatial-frequency content of the generating aperture. In fact, the main advantage of the scheme advocated in this paper is that it allows us to send narrow pulses generated from large apertures to far distances with very little spreading. A static aperture of a fixed radius R generating a narrow Gaussian pulse having a waist $w_0 < R$ would behave as if it had an effective radius equal to the waist of the Gaussian. In this case, the diffraction length of the field generated by that static aperture is $z_R = \pi w_0^2/\lambda$, independent of how large R is. A narrow Gaussian pulse would not go very far before it started to spread out. By contrast, a dynamic aperture is able to send a Gaussian pulse of a very narrow waist to a much larger distance before its amplitude starts to fall off. In fact, we expect the dynamic aperture to extend the half-amplitude range by a factor of R_{max}/w_0. A similar enhancement factor for the range of LW pulses has been deduced in Ref. 24.

To make our arguments more precise, we consider the case of a Gaussian field generated from an aperture having a fixed radius R greater than the waist of the Gaussian w_0. We choose the spectrum of the initial excitation to give $w_0 = \sqrt{a_1/\beta}$, as in the case of our dynamic aperture. The illuminating field is chosen to carry a single frequency $\omega_0/c = 1/a_1$, which is comparable with the bandwidth of our excitation of the FWM aperture. Specifically, we choose

$$\Phi(\chi, \omega) = \frac{\pi}{\beta}\,\delta(\omega - \omega_0)\exp[-(\chi^2/4\beta)a_1], \tag{4.7}$$

and the generated field becomes

$$\Psi(\rho, z, t) = \frac{1}{2\beta}\int_0^\infty d\chi\chi J_0(\chi\rho)\exp[-(\chi^2/4\beta)a_1] \times \exp(i\omega_0 t)\exp[-i\sqrt{(\omega_0/c)^2 - \chi^2}\,z]. \tag{4.8}$$

To be able to compare the performance of such an aperture with that of the dynamic one, we choose the parameters β and a_1 to have the same values, such that $\beta a_1 \ll 1$. In integration (4.8) we have $\chi_{max}^2/(\omega_0/c)^2 = (\beta/a_1)/(1/a_1)^2 = \beta a_1 \ll 1$; thus the paraxial approximation could be introduced into the integrand of Eq. (4.8) such that

$$\exp[-i\sqrt{(\omega_0/c)^2 - \chi^2}\,z \simeq \exp[-i(\omega_0/c)z] \times \exp[+i(\chi^2 c/2\omega_0)z].$$

Using such an approximation together with the substitution $(\omega_0/c) = 1/a_1$ reduces the integration in Eq. (4.8) to

$$\begin{aligned}\Psi(\rho, z, t) &\simeq \frac{1}{2\beta}\int_0^\infty d\chi\chi J_0(\chi\rho)\exp\{-\chi^2[(a_1/4\beta) - i(za_1/2)]\}\exp[-i(z - ct)/a_1] \\ &= \frac{1}{(a_1 - i2\beta a_1 z)}\exp[-\beta\rho^2/(a_1 - i2\beta a_1 z)] \times \exp[-i(z - ct)/a_1].\end{aligned} \tag{4.9}$$

The above expression indicates that the centroid of Ψ, for which $\rho = 0$ and $z = ct$, reaches half its initial

value when $z = 1/2\beta$. Such a range should be compared with the cases considered in Fig. 5, where the dynamic aperture has been characterized by the parameters $a_1 = 4 \times 10^{-7}$ m and $\beta = 400$ m^{-1}. For these parameter values, the centroid of a Gaussian generated by a static aperture decays to half its initial amplitude at a distance $z = 2.5 \times 10^{-3}$ m, independent of $R_{\max}$. In contrast, the half-amplitude range of the equivalent dynamic aperture depends on $R_{\max} \propto cT/\sqrt{\beta a_1}$. Such a dependence extends the half-amplitude ranges to distances of the order of several hundred meters. Furthermore, the amplitude of the Gaussian launched from a static aperture decays to almost one millionth of its initial value when it reaches a distance of $z = 500$ m. At the same position in front of a dynamic aperture the amplitude of the centroid falls off only by a factor of one half.

The difference in the performance of the two apertures reflects the importance of the efficiency by which a Gaussian utilizes the generating capabilities of a specific source. A narrow pulse generated from a static aperture of a much larger radius is completely inefficient. It makes no use whatsoever of the extension of its source, which for all practical purposes performs with an effective radius equal to that of the Gaussian. In contrast, a narrow central Gaussian that is allowed to expand with time such that it fills up the whole extension of its expanding dynamic aperture makes much better use of the size of its source; hence its half-amplitude range depends on $R_{\max}$, and it travels to much larger distances with very little decay. One should emphasize, however, that the case of the dynamic FWM aperture considered here is not the only possible way in which a narrow central pulse is allowed to expand and to fill the extension of its source for all times. One can investigate other possible schemes simply by varying the transverse χ spectral content. This will change the manner by which the illuminating field fills up the aperture as the latter varies its size. One can also study the effect of the rate of expansion of the radius of the source. The FWM aperture considered in this paper has an effective radius that varies linearly with time. It is of interest to study various expansion patterns; for example, a quadratic or a cubic dependence on time is a straightforward extension of the present scheme.

5. CONCLUSIONS

In this paper we have studied the possibility of launching approximations to the FWM pulse from a dynamic Gaussian aperture. The type of aperture investigated varies its effective radius with time. We started by introducing the infinite FWM aperture, which is allowed to shrink from an infinite radius at $t = -\infty$ to its smallest dimension at $t = 0$, and then it expands back to its original infinite size. The excitation of such an aperture utilizes finite power for all times. However, it consumes an infinite amount of energy because it needs to be excited for an infinitely long time. The causal field generated by such an aperture has been calculated by means of Huygen's construction. It has been shown that such a field does not contain any acausal components. The generated field resembles the source-free FWM pulse, which has a highly focused central Gaussian that propagates without any decay. This infinite FWM aperture is an interesting construction in its own right; nevertheless, it is an abstract device that cannot be implemented in reality. On the other hand, a firm comprehension of the different properties of such an ideal source helps us to understand the effects of the various design parameters involved in its finite-time counterpart, which is physically realizable.

The finite-time FWM aperture is excited for a period of time equal to $2T$. It shrinks from its maximum radius at $t = -T$ to its smallest size at $t = 0$ and then expands back to its original size at $t = +T$. We have demonstrated that the narrow central Gaussian generated by such an aperture efficiently utilizes the capabilities of its source. This is the case because the energy of the illumination of the Gaussian aperture is always spread over its entire extension as it expands with time. Notice that for all times other than $t \simeq 0$, the radius of the aperture is much larger than the waist w_0. This scheme was compared with the generation of a Gaussian field from a static aperture. The latter is characterized by a diffraction length that depends only on the waist of the beam w_0 and is independent of the radius R of the aperture, as long as $R > w_0$. We have demonstrated that such a field makes no use whatsoever of the size of its source, and increasing the aperture size does not improve the decay behavior of the generated field. We have also shown that a comparison between the performance of a Gaussian generated from a dynamic aperture and that of a Gaussian launched from a static aperture greatly favors the former case even when both sources use signal generators of comparable frequencies. The dynamic aperture is capable of extending the half-amplitude range up to several orders of magnitude in comparison with the Gaussian beam; thus it provides a unique scheme to send very narrow Gaussians over extended distances of localization. The enhancement over the static case depends primarily on the ratio of $R_{\max}$ to w_0, i.e., the ratio of the maximum aperture radius to the minimum one. It might not be so easy to physically realize an aperture that shrinks from a very large radius to a minuscule one. At the same time, one should recall that in order to generate the central Gaussian pulse we have to choose the β and the a_1 parameters in such a way that the aperture varies its radius at a superluminal speed. This forces us to utilize independently addressable source elements that use signal generators of very large bandwidths in the terahertz range. Such constraints are the reason behind our exaggerated choice of parameter values in Section 4. We resorted to such an excessive selection in order to highlight the possible potential of dynamic Gaussian apertures. Fortunately, the advancement in ultrafast switching optical devices[25] can now provide the needed signal generators that might constitute the independently addressable elements of the advocated dynamic aperture.

Finally, we point out that the present scheme fits together with other procedures that have been proposed to launch approximations to the FWM field.[11,26,27] It has been realized for a while[3] that the FWM field could be generated from a moving complex point source. This fact asserts the dynamic nature of any source adopted to generate approximations to the FWM field. Some approaches resorted to moving physical sources situated on the characteristic of the generated Gaussian beam.[26] In our case the needed dynamic ingredient follows *only* from

the time variation of the radius of the aperture. We have shown that such an approach provides a systematic way to relate the behavior of the propagating FWM Gaussian field to familiar antenna design factors such as the bandwidth of the source generators, the size of the aperture, and the possible coupling between the temporal and the spectral components of the illumination field. No doubt the last factor opens the way for more studies that can achieve further enhancements in the rates of decay and spread of analogous pulsed fields, but much of this effort is beyond the scope of this paper and will be the subject of future research.

REFERENCES

1. A. M. Shaarawi, R. W. Ziolkowski, and I. M. Besieris, "On the evanescent fields and the causality of the focus wave modes," submitted to J. Math. Phys.
2. J. N. Brittingham, "Focus wave modes in homogeneous Maxwell's equations: transverse electric mode," J. Appl. Phys. **54,** 1179–1189 (1983).
3. R. W. Ziolkowski, "Exact solutions of the wave equation with complex source locations," J. Math. Phys. **26,** 861–863 (1985).
4. I. M. Besieris, A. M. Shaarawi, and R. W. Ziolkowski, "A bidirectional traveling plane wave representation of exact solutions of the scalar wave equation," J. Math. Phys. **30,** 1254–1269 (1989).
5. R. W. Ziolkowski, I. M. Besieris, and A. M. Shaarawi, "Aperture realizations of the exact solutions to homogeneous wave equations," J. Opt. Soc. Am. A **10,** 75–87 (1993).
6. P. Hillion, "Spinor focus wave modes," J. Math. Phys. **28,** 1743–1748 (1987).
7. A. M. Shaarawi, I. M. Besieris, and R. W. Ziolkowski, "A novel approach to the synthesis of nondispersive wave packet solutions to the Klein–Gordon and the Dirac equations," J. Math. Phys. **31,** 2511–2519 (1990).
8. A. M. Vengsarkar, I. M. Besieris, A. M. Shaarawi, and R. W. Ziolkowski, "Closed-form, localized wave solutions in optical fiber waveguides," J. Opt. Soc. Am. A **9,** 937–949 (1992).
9. M. K. Tippet and R. W. Ziolkowski, "A bidirectional wave transformation of the cold plasma equations," J. Math. Phys. **32,** 488–492 (1991).
10. R. Donnelly and R. W. Ziolkowski, "A method of constructing solutions of homogeneous partial differential equations: localized waves," Proc. R. Soc. London Ser. A **437,** 673–692 (1992).
11. R. W. Ziolkowski, "Localized transmission of electromagnetic energy," Phys. Rev. A **39,** 2005–2033 (1989).
12. A. M. Shaarawi, I. M. Besieris, and R. W. Ziolkowski, "Localized energy pulse trains launched from an open, semi-infinite, circular waveguide," J. Appl. Phys. **65,** 805–813 (1989).
13. R. W. Ziolkowski, I. M. Besieris, and A. M. Shaarawi, "Localized wave representations of acoustic and electromagnetic radiation," Proc. IEEE **79,** 1371–1378 (1991).
14. R. W. Ziolkowski, "Properties of electromagnetic beams generated by ultra-wide bandwidth pulse-driven arrays," IEEE Trans. Antennas Propag. **40,** 888–905 (1992).
15. R. W. Ziolkowski and J. B. Judkins, "Propagation characteristics of ultrawide-bandwidth pulsed Gaussian beams," J. Opt. Soc. Am. A **9,** 2021–2030 (1992).
16. R. W. Ziolkowski, D. K. Lewis, and B. D. Cook, "Experimental verification of the localized wave transmission effect," Phys. Rev. Lett. **62,** 147–150 (1989).
17. R. W. Ziolkowski and D. K. Lewis, "Verification of the localized wave transmission effect," J. Appl. Phys. **68,** 6083–6086 (1990).
18. B. Hafizi and P. Sprangle, "Diffraction effects in directed radiation beams," J. Opt. Soc. Am. A **8,** 705–717 (1991).
19. J. Durnin, J. J. Miceli, Jr., and J. H. Eberly, "Diffraction-free beams," Phys. Rev. Lett. **58,** 1499–1501 (1987).
20. E. Heyman, "Focus wave modes: a dilemma with causality," IEEE Trans. Antennas Propag. **37,** 1604–1608 (1989).
21. E. Heyman, B. Z. Steinberg, and L. B. Felsen, "Spectral analysis of focus wave modes," J. Opt. Soc. Am. A **4,** 2081–2091 (1987).
22. P. M. Morse and H. Feshbach, *Methods of Theoretical Physics* (McGraw-Hill, New York, 1953), Sec. 11.3.
23. M. Abramowitz and I. A. Stegun, *Handbook of Mathematical Functions* (Dover, New York, 1972).
24. R. W. Ziolkowski, "Localized wave physics and engineering," Phys. Rev. A **44,** 3960–3984 (1991).
25. N. Froberg, M. Mack, B. B. Hu, X.-C. Zhang, and D. H. Auston, "500 GHz electrically steerable photoconducting antenna array," Appl. Phys. Lett. **58,** 446–448 (1991).
26. P. Hillion, "Approximation of the scalar focus wave modes," J. Opt. Soc. Am. A **9,** 137–141 (1992).
27. A. Wunsche, "Embedding of focus wave modes into a wider class of approximate wave equation solutions," J. Opt. Soc. Am. A **6,** 1661–1668 (1989).